

Predicting solid solubility in CoCrFeNiM_x (M = 4d transition metal) high-entropy alloys

Saad Sheikh,¹ Huahai Mao,^{2,3} and Sheng Guo^{1,a)}

¹Materials and Manufacturing Technology, Chalmers University of Technology, SE-41296 Göteborg, Sweden

²Materials Science and Engineering, KTH Royal Institute of Technology, Brinellvägen 23, SE-100 44 Stockholm, Sweden

³Thermo-Calc Software AB, Råsundavägen 18A, SE-169 67 Stockholm, Sweden

(Received 17 February 2017; accepted 7 May 2017; published online 19 May 2017)

CoCrFeMnNi is a prototype fcc-structured high-entropy alloy. Numerous efforts have been paid to strengthen CoCrFeMnNi, by replacing Mn with other elements for an enhancement of the solid solution strengthening. 4d transition metals, including Zr, Nb, and Mo, are of interest for this purpose, since they have much larger atomic radii than that of Mn. However, Nb and Mo are known to have a low solid solubility in fcc-structured CoCrFeNi. Compared to Nb and Mo, Zr has an even larger atomic radius. The solid solubility of Zr in fcc-structured CoCrFeNi was investigated in this work, combining both experimental studies and thermodynamic calculations. In addition, based on previous results and new results obtained here, methods to predict the solid solubility in CoCrFeNiM_x (M = Zr, Nb, and Mo) alloys were developed. Particularly, the average d-orbital energy level, *Md*, was re-evaluated in the present work, for an improved predictability of the solid solubility in fcc-structured high entropy alloys containing 4d transition metals. *Published by AIP Publishing.* [<http://dx.doi.org/10.1063/1.4983762>]

I. INTRODUCTION

High entropy alloys (HEAs), or multi-principal-element alloys, have gained ever-increasing attention from metallic materials related academia and industries since the term was first proposed in 2004.^{1,2} On the one hand, the new alloy design strategy enables the opening of a vast unexplored compositional space and therefore the possibility of developing new alloys with unprecedented structural and functional properties.^{3–7} Particularly, exploring the potential of utilizing HEAs as a new generation of ultrahigh-temperature materials^{8–10} and irradiation resistant materials^{11–13} has been intensively pursued recently. On the other hand, HEAs do not behave much different to conventional alloys in terms of their mechanical behavior and typically on the strength-ductility trade off.^{3,14} In general, for solid solution forming HEAs, fcc structured HEAs are ductile but low in strength, while bcc structured HEAs can have higher strength but are accompanied by low ductility (note that bcc structured HEAs can also be ductile but these ductile bcc HEAs have relatively low strength compared to those brittle ones⁸); precipitation of intermetallic compounds in both fcc and bcc structured HEAs can lead to strengthening but it quite often also leads to embrittlement. Numerous efforts have been dedicated to break the trade-off between strength and ductility in HEAs,¹⁵ but it remains to be a great challenge for most alloy systems.

During the past two decades since the advent of HEAs, partially due to the lack of robust alloy design principles, most developed HEAs are derivatives of prototype HEAs, namely, fcc structured CoCrFeMnNi² and bcc structured MoNbTaVW¹⁰ and HfNbTaTiZr¹⁶ (as shown in Table I, it is interesting to note that the constituent elements in these prototype HEAs are all

neighboring elements in the periodic table). Survey of the literature clearly indicates that, comparatively, there exist more efforts to strengthen fcc structured alloys than to ductilize bcc structured alloys, to address the above mentioned strength-ductility trade-off in HEAs. As an example, CoCrFeMnNi has been the most intensively studied fcc structured HEA, which is now well-known for its outstanding mechanical performance at cryogenic temperatures.¹⁷ CoCrFeMnNi has very decent ductility but its strength is relatively low. Among different efforts to design stronger alloys than CoCrFeMnNi, replacing Mn by other elements and particularly elements with a larger atomic radius than Mn (refer to Table I) seems to be a straightforward route. The idea is to enhance the solid solution strengthening resulting from the solid solutioning of large atoms (Co, Cr, Fe, and Ni have close atomic radii¹⁸) and at the same time to avoid the precipitation of other phases such as intermetallic compounds by not surpassing the solid solubility range of large atoms in the fcc phase. Here in this work, we aim to study the solid solutioning in CoCrFeNiM_x HEAs, where M are 4d transition metals Zr, Nb, and Mo. We choose to study the replacement of Mn by Zr, Nb, and Mo based on three considerations. First, they all have a larger atomic radius than that of Mn, and so, they can potentially result in alloys stronger than CoCrFeMnNi. Second, from previous work, Nb and Mo are known to have low solid solubility in CoCrFeNiNb_x^{19,20} and CoCrFeNiMo_x^{21,22} alloys. It would be interesting to see how much of another 4d element, Zr, with an even larger atomic radius than Nb and Mo, can be dissolved in CoCrFeNiZr_x alloys. Third, we recently²³ showed that the average energy of d-orbital levels, *Md*, can be used to effectively predict the solid solubility limit in fcc structured HEAs containing 3d transition metals, but it encounters problems when 4d transition metals are alloyed. This work then

^{a)} Author to whom correspondence should be addressed: sheng.guo@chalmers.se

TABLE I. Excerpt of the periodic table listing typical transition metals that are commonly used in high-entropy alloys. For each element, its atomic number and atomic radius (in Å)¹⁸ are given. The two shaded series of elements, Cr-Mn-Fe-Co-Ni and V-Nb-Ta-Mo-W, indicate one prototype fcc-structured equiatomic CoCrFeMnNi alloy and one prototype bcc-structured equiatomic MoNbTaVW high entropy alloy, and the location of constituent elements in the periodic table.

3d	22	23	24	25	26	27	28	29
	Ti	V	Cr	Mn	Fe	Co	Ni	Cu
	1.462	1.316	1.249	1.350	1.241	1.251	1.246	1.278
4d	40	41	42	43	44	45	46	47
	Zr	Nb	Mo	Tc	Ru	Rh	Pd	Ag
	1.603	1.429	1.363					
5d	72	73	74	75	76	77	78	79
	Hf	Ta	W	Re	Os	Ir	Pt	Au
	1.578	1.430	1.367					

provides another opportunity to revisit the problem and look for solutions, by inspecting the connection between Md and the solid solubility of 4d transition metal elements Zr, Nb, and Mo, in fcc structured CoCrFeNiM_x HEAs ($M = \text{Zr, Nb, and Mo}$). It has to be noted here that the motivation of the current work originates from the intention to address the strength-ductility trade-off in HEAs and particularly in fcc structured HEAs, but in the end we end up in discussing the solid solubility of 4d transition metals, Zr, Nb and Mo, in typical fcc structured HEAs, CoCrFeNi . The work presented here, therefore, is certainly relevant but essentially not directly addressing the strength-ductility trade-off in HEAs.

II. EXPERIMENTAL METHODS AND THERMODYNAMIC CALCULATIONS

A series of CoCrFeNiZr_x ($x = 0.05, 0.1, 0.15, 0.2, 0.25, 0.3, 0.35, 0.4, 0.45, \text{ and } 0.5$, in atomic portion) HEAs were prepared for this work. The alloy preparation was carried out using high purity (>99.9%) elemental materials by arc melting on a water-cooled copper plate in a Ti-gettered Ar atmosphere. The arc-melted ingot was flipped and re-melted at least five times to ensure thorough chemical homogeneity. The drop-cast ingots have a diameter of 10 mm and a length of 90 mm. The crystal structure of the alloy was examined by using a Bruker AXS D8 advance X-ray diffraction (XRD) system using Cr-K_α radiation. The microstructure and chemical composition of the as-cast sample were studied on a polished and chemically etched specimen using a LEO Gemini 1550 scanning electron microscope (SEM), equipped with an energy dispersive spectrometer (EDS). The etchant used to reveal the microstructure was the commercially available Electrolyte A2 (Struers, Denmark).

The purpose of the experiments is to determine how much Zr can be dissolved in CoCrFeNiZr_x alloys, judging mainly from the XRD and microstructure. Apart from the experimental study, thermodynamic calculations based on the CALPHAD-type database were also carried out for the prediction of Zr solubility in the CoCrFeNiZr_x HEAs and corresponding phase relations. CALPHAD is the acronym for CALculation of PHase Diagrams. Using the CALPHAD approach which couples phase diagram and thermodynamic

property information, a special thermodynamic database, TCHEA1, was developed at Thermo-Calc^{24,25} for HEAs. Based on the principle of Gibbs energy minimization the software, Thermo-Calc has been widely used to evaluate the phase equilibria and phase transformations in complex multi-component alloy systems, including HEAs.²⁶⁻³¹ The TCHEA1 database is essentially established based on the TCNI database which was mainly applied for Ni-based alloys. However, in TCHEA1 all binary systems and many key ternary systems including all possible phases were thermodynamically assessed in full composition range. Moreover, during the development of the database, high throughput DFT calculations were employed to check the mixing enthalpy data for solid solutions (especially in metastable compositional ranges) and formation enthalpy data for intermetallic phases (especially for metastable end-members). It may be said that all possible phases are included, at least for the present case, in the database. In this work, phase relations and equilibrium phase fractions varying with temperature were calculated using the TCHEA1 database for the CoCrFeNiZr_x HEAs.

III. SOLID SOLUTIONING IN CoCrFeNiZr_x HEAs

Figure 1 shows the XRD patterns for as-cast CoCrFeNiZr_x alloys that were prepared in this work. For $x = 0.05$ and 0.1 , the XRD patterns seem to contain mainly the fcc solid solution phase plus a small amount of the Ni_7Zr_2 phase. From $x = 0.15$ to $x = 0.4$, the XRD results indicate the existence of three phases, namely, the fcc solid solution phase, the Ni_7Zr_2 phase, and the Co_2Zr -like C15 Laves phase. The amount of the C15 Laves phase at $x = 0.15$ and the amount of the Ni_7Zr_2 phase at $x = 0.4$ are negligible judging from their weak peak intensities. For $x = 0.45$ and 0.5 , the XRD patterns show only two phases, the fcc solid solution phase and the C15 Laves phase. The XRD results indicate that Zr has almost no solid solubility in CoCrFeNiZr_x alloys, with additional details of EDS measurements provided in Table II. Certainly, XRD results cannot tell all information in such compositionally complex alloy systems, such as ordering and heterogeneity. However, they are sufficient for the

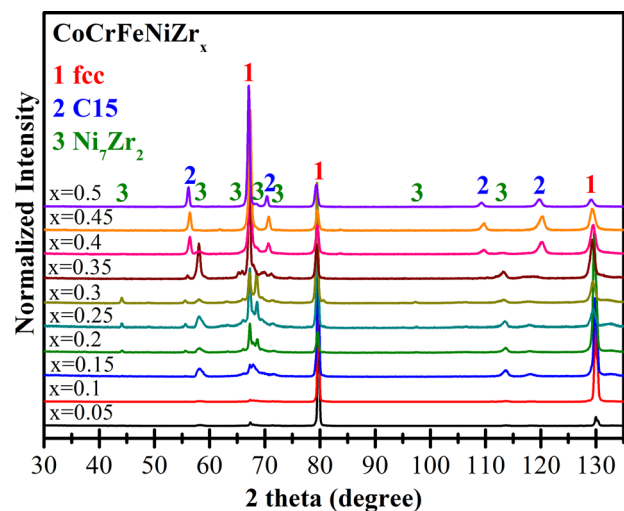


FIG. 1. XRD patterns for CoCrFeNiZr_x alloys that were prepared in this work.

TABLE II. EDS analysis on the chemical compositions of the fcc solid solution phase in as-cast CoCrFeNiZr_x HEAs.

Alloy Composition		Element (at. %)				
CoCrFeNiZr_{0.1}		Co	Cr	Fe	Ni	Zr
Nominal		24.39	24.39	24.39	24.39	2.44
fcc phase		25.20	26.27	26.4	22.02	0.11
CoCrFeNiZr_{0.15}		Co	Cr	Fe	Ni	Zr
Nominal		24.10	24.10	24.10	24.10	3.61
fcc phase		24.98	27.16	26.87	20.87	0.12
CoCrFeNiZr_{0.2}		Co	Cr	Fe	Ni	Zr
Nominal		23.81	23.81	23.81	23.81	4.76
fcc phase		24.54	28.18	27.36	19.73	0.19
CoCrFeNiZr_{0.25}		Co	Cr	Fe	Ni	Zr
Nominal		23.53	23.53	23.53	23.53	5.88
fcc phase		24.24	29.02	27.91	18.65	0.18
CoCrFeNiZr_{0.3}		Co	Cr	Fe	Ni	Zr
Nominal		23.26	23.26	23.26	23.26	6.98
fcc phase		23.90	28.52	27.28	18.69	1.61
CoCrFeNiZr_{0.35}		Co	Cr	Fe	Ni	Zr
Nominal		22.99	22.99	22.99	22.99	8.05
fcc phase		23.60	31.08	28.53	16.58	0.21

purpose of discussing the solid solubility in HEAs, if they can be complemented by other information, for example, thermodynamic calculations. Indeed, the XRD results are in excellent agreement with what is predicted by thermodynamic calculations (Fig. 2). Fig. 2(a) shows the predicted phase equilibria in the isoplethic section of CoCrFeNiZr_x, i.e., the vertical section along the joint of CoCrFeNi-CoCrFeNiZr. The homogeneity range of the fcc solid solution is calculated being extremely narrow extending from the CoCrFeNi side. In particular, the experimentally observed phase assemblages for the CoCrFeNiZr_x alloys agree reasonably well with the calculated phase equilibria. With the increase in the Zr content in CoCrFeNiZr_x, i.e., the x value from 0 to 0.5, the fcc solid solution is always the primary phase. However, the secondary phase changes from Ni₇Zr₂ at low Zr HEAs to the C15 Laves phase at higher Zr. These phases stable above the solidus are usually observed in as-cast HEAs,²⁶ which is verified in the present case for the CoCrFeNiZr_x alloys. During the cooling, for x = 0.05, 0.1, and 0.15, fcc is the first phase precipitated from the melt, followed by the secondary phase Ni₇Zr₂. The amounts of the equilibrium phases and the accumulated solid phases during casting at different temperatures are illustrated in Figs. 2(b) and 2(c), respectively, for some of the CoCrFeNiZr_x alloys (x = 0.05, 0.15, 0.3, 0.4, and 0.5). At x = 0.05 fcc is the dominant solid phase while Ni₇Zr₂ having a very minor fraction, which was confirmed in both the abovementioned XRD study (Fig. 1) in terms of peak positions for the crystal structure and peak intensities for the relative content, and the following microstructure study by means of SEM-EDS. At x = 0.15, a considerable amount of the Ni₇Zr₂ phase is expected during the solidification. At x = 0.30, three solid phases fcc + Ni₇Zr₂ + C15 will form during the casting. For x = 0.4 and 0.5, the Ni₇Zr₂ phase is absent according to the equilibrium calculations; instead, one may expect a dual-phase microstructure of fcc + C15 in the as-cast alloys. It is

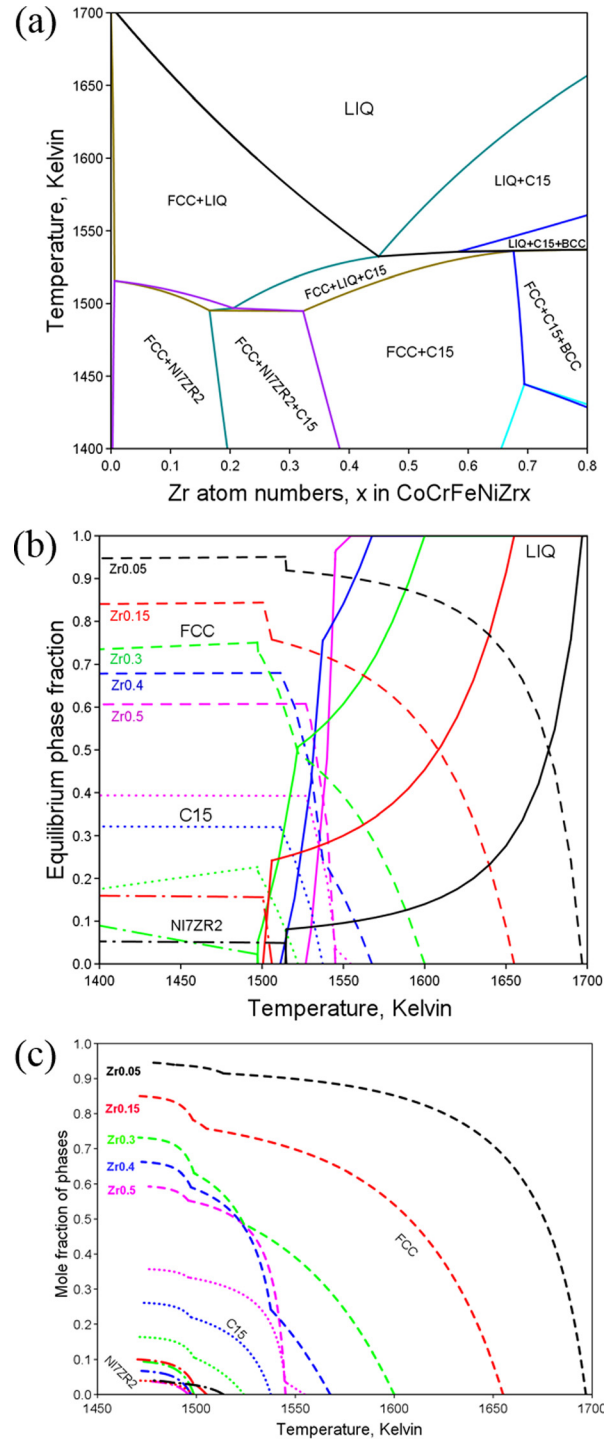


FIG. 2. Thermodynamic calculations of the CoCrFeNiZr_x alloys. (a) Phase equilibria in the vertical section of CoCrFeNiZr_x. (b) Calculated equilibrium phase fraction, in mole, at various temperatures and alloy compositions with different Zr contents. (c) Predicted solid phase fraction, in mole, by Scheil simulation of alloys with different Zr contents. The black curves represent the CoCrFeNiZr_{0.05} alloy, red for CoCrFeNiZr_{0.15}, green for CoCrFeNiZr_{0.3}, blue for CoCrFeNiZr_{0.4}, and pink for CoCrFeNiZr_{0.5}. The fractions of the liquid phase are plotted in solid curves, FCC in dashed curves, C15 Laves in dotted curves, and Ni₇Zr₂ in dashed-dotted curves.

interesting to notice in Figs. 2(b) and 2(c) that at x = 0.5 the fcc and C15 Laves phase start precipitating at very close temperatures. It implies that the composition CoCrFeNiZr_{0.5} is quite close to the eutectic point (check Fig. 2(a) as well),

which was verified by the present microstructure investigation given below. In summary, thermodynamic equilibrium calculations using TCHEA1 agree very well with our experimental information. One has to keep in mind that such calculations were performed on the assumption of the full equilibrium state; moreover, no kinetic factors were taken into account in this work. For example, at $x = 0.4$ our XRD result showed a minor amount of Ni_7Zr_2 ; however, this phase was not predicted being precipitated from the liquid according to our equilibrium calculations. In order to better understand the solidification process and compare with the experimental information, we performed the Scheil simulation which assumes that the diffusion in liquid is sufficiently fast while that in solid phases is negligible. The liquid composition changes gradually during solidification. For the

alloy at $x = 0.4$, the Scheil simulation predicts a minor amount of Ni_7Zr_2 , which agrees well with our experimental observation. One may consider that the global equilibrium calculation and the Scheil simulation mimic two extreme conditions for the solidification process. A real case should happen at the condition in between.

The microstructures for as-cast CoCrFeNiZr_x HEAs, as shown in Fig. 3, also support the conclusion from both experimental observations and thermodynamic calculations in that Zr has almost no solid solubility in CoCrFeNi . Even at $x = 0.05$, new phases other than the fcc solid solution, which appears as the smooth cellular structure, can be observed. Combining results from XRD and thermodynamic calculations, the structure formed at the boundaries among cellular fcc phases corresponds to the mixed fcc phase and

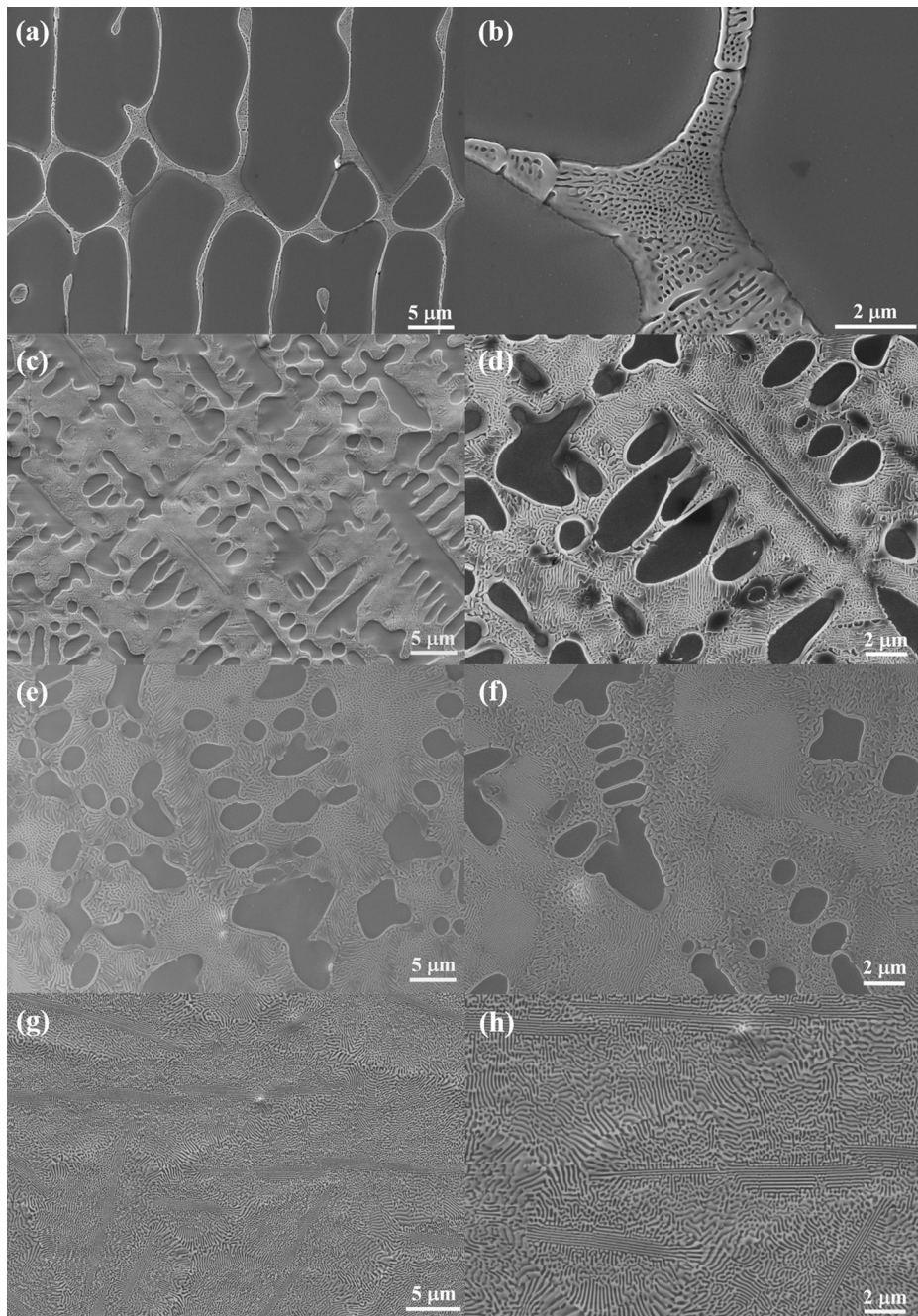


FIG. 3. Representative microstructures of CoCrFeNiZr_x alloys. (a) and (b) $x = 0.05$; (c) and (d) $x = 0.3$; (e) and (f) $x = 0.4$; and (g) and (h) $x = 0.5$.

the Ni_7Zr_2 phase. At $x=0.3$, the amount of the fcc phase decreases sharply compared to that at $x=0.05$ (check the calculated Fig. 2(b) as well), and the morphology of the fcc phase becomes less regular. Halo formation can be clearly seen surrounding the fcc phase. Apart from the fcc phase, the remaining microstructure appears to be multi-phase and it shall comprise a mixture of the C15 Laves phase, the fcc phase, and also the Ni_7Zr_2 phase. At $x=0.4$, the microstructure very much resembles the near-eutectic microstructure where the primary fcc phase is again surrounded by halos, and the lamellar eutectic microstructure is formed by the alternatively grown C15 Laves phase and the fcc phase. According to XRD results, the Ni_7Zr_2 phase remains to exist at $x=0.4$ but has a quite low amount and is difficult to be identified in the microstructure. At $x=0.5$, an almost fully eutectic lamellar structure formed by the C15 Laves phase and the fcc phase is clearly seen, which agrees nicely with thermodynamic calculations. Table II lists the EDS results, which very importantly shows that Zr almost does not dissolve in the fcc phase at all. Using TCHEA1, the Zr solubility in the fcc phase equilibrium at 1500 K was predicted as 0.15, 0.17, 0.18, 0.18, 0.18, and 0.19 at. % for the CoCrFeNiZr_x alloys at $x=0.1, 0.15, 0.2, 0.25, 0.3,$ and 0.35 , respectively.

IV. PREDICTION OF SOLID SOLUBILITY IN CoCrFeNiM_x ($M = 4\text{D TRANSITION METAL}$) HEAs

A. The two-parameter $\delta-\Delta H_{\text{mix}}$ approach

Considering the compositional complexity of HEAs and the possibility of forming different phases in HEAs, i.e., solid solution phases, intermetallic compounds, or even the amorphous phase, the alloy design principles for HEAs have always been an intensively studied topic.^{32–36} Although the high configuration entropy can help to stabilize the formation of solid solutions in HEAs, it is now known that it is neither a necessary nor a sufficient condition for the solid solution formation.^{37,38} In many alloy systems where alloys do have the multi-principal-element compositional complexity, they do not form solid solutions or purely solid solutions, and intermetallic compounds can form. The capability of a theoretical, semi-theoretical, or even empirical way to predict the solid solubility and importantly to avoid the formation of intermetallic compounds is much desired, from both the fundamental science perspective, to understand the solid solubility in such compositionally complicated alloy systems, and the practical engineering application perspective, since the mechanical behavior of solid solution forming HEAs and intermetallic compounds forming HEAs can differ to a large extent.

As we show here, theoretical methods like CALPHAD can certainly be used to predict the phase formation in HEAs. However, practically it is also necessary to develop empirical or semi-empirical methods for the alloy design, since they are easier to use, cheaper to apply (no need for special software and databases), and faster to calculate. Among the existing empirical rules to predict the phase formation in HEAs, the two-parameter approach, $\delta-\Delta H_{\text{mix}}$, probably receives the most attention due to its easy definition

and calculation.^{32–34} δ aims to describe the atomic size mismatch among constituent elements, and it is given by $\delta = \sqrt{\sum_{i=1}^n c_i (1 - r_i / \sum_{j=1}^n c_j r_j)^2}$, where n is the number of alloying elements, c_i is the atomic percentage for the i th element, and r_i or r_j is the atomic radius for the i th or j th component. ΔH_{mix} tries to use one parameter to describe the weight averaged mixing enthalpy of all pairs of constituent elements in the alloy and is given by $\Delta H_{\text{mix}} = \sum_{i=1, j>i}^n 4\Delta H_{AB}^{\text{mix}} c_i c_j$, where $\Delta H_{AB}^{\text{mix}}$ is the enthalpy of mixing for the binary equiatomic AB alloys. As shown in Fig. 4, using the two-parameter $\delta-\Delta H_{\text{mix}}$ approach, the formation of solid solutions can be conveniently predicted when δ is small ($\delta < 0.066$), and ΔH_{mix} is insignificantly negative or slightly positive ($-11.6 < \Delta H_{\text{mix}} < 3.2$ kJ/mol). However, the problem is that in this range of $\delta-\Delta H_{\text{mix}}$, intermetallic compounds can also form. In other words, this $\delta-\Delta H_{\text{mix}}$ approach provides necessary but not sufficient conditions for the solid solution formation in HEAs. As shown in Fig. 4, when using $\delta-\Delta H_{\text{mix}}$ to predict the phase formation for CoCrFeNiZr_x alloys, half of the prepared alloys are predicted to form solid solutions. However, both experimental results and thermodynamic calculations confirm that intermetallic compounds form in all prepared CoCrFeNiZr_x alloys. Therefore, the question is that, how can one more accurately predict the phase formation in CoCrFeNiZr_x HEAs?

B. The improved $\delta-\Delta H_{\text{mix}}$ approach

Quinary CoCrFeMnNi is the prototype fcc structured HEA, and it is correctly predicted by the $\delta-\Delta H_{\text{mix}}$ approach to form the solid solution phase, as shown in Fig. 4. It is known from this work that CoCrFeNiZr_x alloys can almost not form the fcc solid solution, since intermetallic compounds form even at very low Zr concentrations. However, not forming solid solutions for CoCrFeNiZr_x alloys is incorrectly reflected in Fig. 4. The problem essentially originates from the definition of ΔH_{mix} used in the $\delta-\Delta H_{\text{mix}}$ approach. ΔH_{mix} is conveniently defined as the weight averaged mixing enthalpy of all paired constituent elements in the alloy.

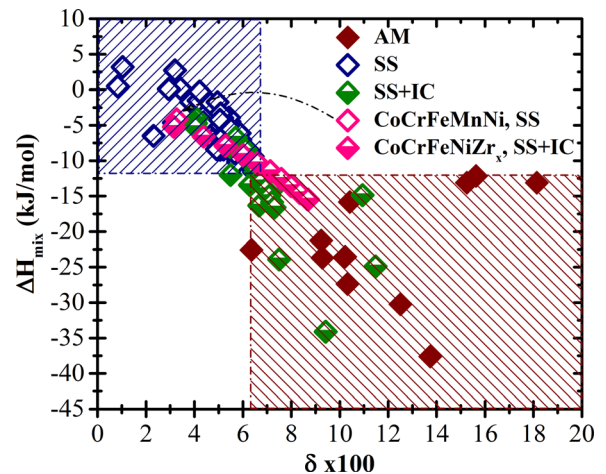


FIG. 4. The two-dimensional $\delta-\Delta H_{\text{mix}}$ plot delineating the phase formation in HEAs, including CoCrFeMnNi and CoCrFeNiZr_x alloys. Data other than CoCrFeMnNi and CoCrFeNiZr_x alloys are taken from Ref. 32.

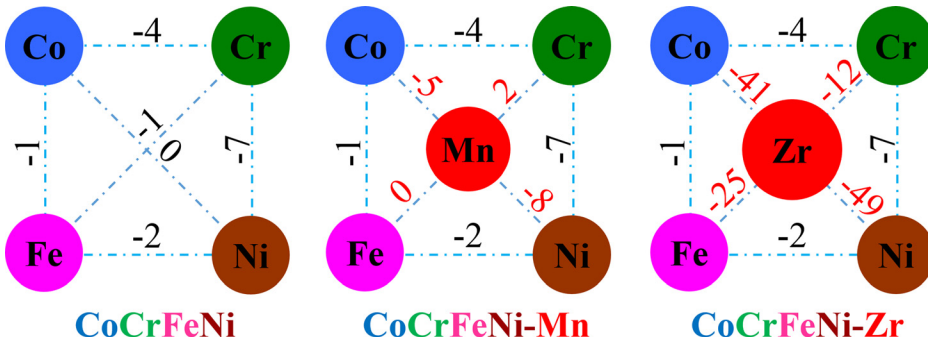


FIG. 5. Mixing enthalpy for binary equiatomic alloys in CoCrFeNi, CoCrFeNiMn, and CoCrFeNiZr.³⁹

However, it is the mixing enthalpy for an individual pair of elements that determines the formation of intermetallic compounds, and such a weight averaging can essentially annihilate the outstanding, very negative mixing enthalpy from a particular pair of elements. Using CoCrFeMnNi as a reference, although ΔH_{mix} for low-Zr CoCrFeNiZr_x alloys can be close to that for CoCrFeMnNi, as shown in Fig. 4, ΔH_{AB}^{mix} for atomic pairs in CoCrFeNiZr_x alloys are much more negative than those in CoCrFeMnNi, as shown in Fig. 5, particularly for the Zr-Ni (−49 kJ/mol) and Zr-Co (−41 kJ/mol) pair.³⁹ Therefore, in spite of the within-the-range ΔH_{mix} for these low-Zr CoCrFeNiZr_x alloys, intermetallic compounds can still form. Noticeably, the formed intermetallic compounds in them are Ni₇Zr₂ and Co₂Zr-like C15 Laves phase, further lending support to the argument that it is the very negative mixing enthalpy from individual atomic pairs, rather than the weight averaged ΔH_{mix} that determines the intermetallic compound formation. How can ΔH_{mix} be improved to reflect the outstanding contribution from the very negative mixing enthalpy from individual atomic pairs, while at the same reflecting the mixing enthalpy of the alloy as a whole (the weight average works well for the latter purpose)?

A primitive thinking would be to increase the weight of the very negative mixing enthalpy from individual atomic pairs, when doing the averaging for the alloy. An easy way of doing this is to use a high order of ΔH_{AB}^{mix} , ΔH_{AB}^{pmix} , to replace ΔH_{AB}^{mix} when calculating ΔH_{mix} . p has to be an odd number to maintain the negative value of ΔH_{AB}^{mix} and certainly p is larger than 1. By replacing ΔH_{AB}^{mix} with ΔH_{AB}^{pmix} , ΔH_{mix} (assuming they are all negative) for all alloys will become more negative. Those intermetallic compound forming alloys, using CoCrFeNiZr_x alloys as an example, however, will have a much more negative ΔH_{mix} , due to the much increased contribution of the very negative mixing enthalpy from individual atomic pairs (Zr-Ni and Zr-Co for CoCrFeNiZr_x alloys) than that of solid solution forming alloys, using CoCrFeMnNi as an example. Therefore, it is expected that the formation of solid solution and intermetallic compounds can be better separated on the two-dimensional δ - ΔH_{mix} plot. This scenario is indeed shown in Fig. 6, when assigning $p = 3$, so $\Delta H_{mix} = \sum_{i=1, j>i}^n 4\Delta H_{AB}^{3mix} c_i c_j$. In the new δ - ΔH_{mix} region where solid solutions including CoCrFeMnNi are formed, almost no intermetallic compounds are seen, although a few exceptions still exist. If one compares Figs. 6 and 4, it is immediately perceived that the newly defined ΔH_{mix} can much better separate the formation of solid solutions and intermetallic compounds using the δ - ΔH_{mix} approach. Certainly, the choice of 3 for p is arbitrary and p can be 5 or 7

or larger odd numbers, but it will not affect the conclusion much.

C. Using Md to predict solid solubility in CoCrFeNiM_x (M = 4d transition metal) HEAs

The improved δ - ΔH_{mix} approach could provide a new method to more accurately predict the phase formation in HEAs. However, the improvement is essentially based on a simple mathematical treatment and its physical meaning is not robust. As shown in Fig. 6, compared to the original δ - ΔH_{mix} approach, the improved one works much better in separating the formation of solid solutions and intermetallic compounds, but still some exceptions exist. Indeed, for alloy systems where intermetallic compounds tend to form and there exists no very negative mixing enthalpy from individual atomic pairs, the improvement of the δ - ΔH_{mix} approach by using the high order of ΔH_{AB}^{mix} will be limited. An example is CoCrFeNiMo_x alloys with known limited Mo solid solubility in CoCrFeNi, but Mo has moderately negative mixing enthalpy with all other elements: −5 kJ/mol for Mo-Co, 0 for Mo-Cr, −2 kJ/mol for Mo-Fe, and −7 kJ/mol for Mo-Ni,³⁹ which is quite close to that in CoCrFeNiMn_x alloys (refer to Fig. 5), but Mn certainly has a higher solid solubility than Mo in CoCrFeNi. Naturally, a more physically robust and more accurate method is desired to predict the solid solubility in HEAs, and specifically in our target CoCrFeNiM_x (M = Zr, Nb, and Mo) alloys.

Previously, we used a single parameter, the average energy of d-orbital levels, Md , to predict the solid solubility, and more specifically the phase boundaries between fcc/bcc

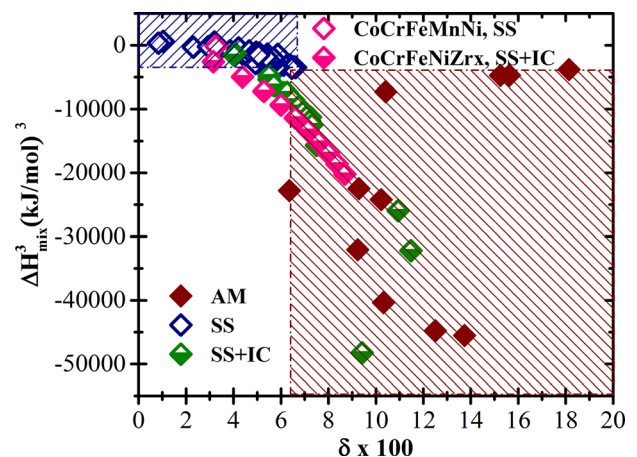


FIG. 6. The improved two-dimensional δ - ΔH_{mix} plot, by replacing ΔH_{AB}^{mix} with ΔH_{AB}^{3mix} when calculating ΔH_{mix} .

solid solution and topological/geometrical closely packed (TCP/GCP) phases in HEAs.²³ The Md parameter can work nicely to predict the solid solubility in fcc structured HEAs containing only 3d transition metals (Table I) and also the solid solubility in bcc structured HEAs. However, the Md parameter does not work well for fcc structured HEAs when 4d transition metals are alloyed, and the reason was attributed to the large bond strength of 4d elements. For fcc structured HEAs containing only 3d transition metals, a critical Md of 0.97 was identified below which the fcc solid solution forms, and beyond which TCP/GCP phases start to form. When 4d transition metals are alloyed, it was found that TCP/GCP phases can form at Md lower than 0.97, such that there exists no critical Md to predict the solid solubility limit. By re-inspecting the data point leading to the above conclusion (Fig. 3 in Ref. 23), it is found that TCP/GCP phases already formed in the supposedly fcc solid solution. In other words, TCP/GCP phases form at lower Md than 0.97, but it could possibly only indicate that the critical Md is lower than 0.97, when 4d transition metals are alloyed. With this thinking in mind, the phase constitutions and corresponding Md for CoCrFeNi and CoCrFeNiM_x (M = Zr, Nb, Mo; Ti, Mn, Cu) HEAs are listed in Table III and plotted in Fig. 7. Apart from 4d transition metals Zr, Nb, and Mo, 3d transition metals Ti, Mn and Cu are also included, to reveal the

phase boundary between the fcc solid solution and intermetallic compounds, including the TCP phase and the Ni₇Zr₂ phase. As shown in Fig. 7, there does seem to exist a critical Md of ~ 0.89 that delineates the phase boundary between the fcc solid solution and intermetallic compounds. The significance of Fig. 7 is at least two-fold. First, it means that the Md parameter can work well to predict the solid solubility in HEAs even when 4d transition metals are alloyed, at least for CoCrFeNiM_x (M = Zr, Nb, and Mo) alloys. Second, Md can possibly be used to predict the phase boundary between the fcc solid solution and intermetallic compounds beyond TCP/GCP phases, as is the case for the Ni₇Zr₂ phase in this work. It is noted that care has to be taken when applying Md to HEAs, as we clarified in our previous work,²³ and the threshold Md to distinguish the formation of solid solutions and TCP/GCP phases or intermetallic compounds can vary depending on the alloy systems and the choice of the base element. Nevertheless, if it is used in the right way, Md can act as an excellent alloy design criterion for HEAs, as have been evidenced here and in our previous work.²³

V. CONCLUSIONS

Efforts to strengthen the ductile but not very strong fcc-structured CoCrFeMnNi HEA were made, by replacing Mn with different amounts of Zr in this work, hoping to enhance the solid solution strengthening by the dissolution of larger atoms in the fcc-structured CoCrFeNi. However, both experimental results and thermodynamic calculations reveal that Zr has almost no solid solubility in CoCrFeNi and an fcc solid solution cannot form in CoCrFeNiZr_x alloys. In addition to Zr, the other two 4d transition metals, Nb and Mo, also have a low solid solubility in CoCrFeNi. Methods to predict the solid solubility in CoCrFeNiM_x (M = Zr, Nb, and Mo) alloys were developed in this work. An improved $\delta - \Delta H_{mix}$ approach, by using a high order of mixing enthalpy from equiatomic binary alloys when calculating the weight averaged mixing enthalpy of all paired constituent elements

TABLE III. Phase constitutions and the d-orbital energy level, Md , in CoCrFeNiM_x (M = Mo, Nb, Zr) HEAs. To reveal the phase boundary, phase constitutions and Md for CoCrFeNi and CoCrFeNiM_x (M = Ti, Mn, Cu) are also listed.

Alloy system	Phase	Md	Reference
CoCrFeNi	fcc	0.874	40
CoCrFeNiCu _{0.5} (3d)	fcc	0.845	41
CoCrFeNiCu (3d)	fcc	0.822	42
CoCrFeNiMn (3d)	fcc	0.890	2
CoCrFeNiMo _{0.1} (4d)	fcc	0.890	21
CoCrFeNiTi _{0.3} (3d) ^a	fcc+ σ +R	0.971	43
CoCrFeNiTi _{0.5} (3d)	fcc+ σ +Laves+R	1.029	43
CoCrFeNiMo _{0.3} (4d) ^a	fcc+ σ	0.921	22
CoCrFeNiMo _{0.5} (4d)	fcc+ σ	0.949	22
CoCrFeNiMo _{0.85} (4d)	fcc+ σ + μ	0.992	22
CoCrFeNiNb _{0.103} (4d)	fcc+Laves	0.905	19
CoCrFeNiNb _{0.155} (4d)	fcc+Laves	0.920	19
CoCrFeNiNb _{0.206} (4d)	fcc+Laves	0.934	19
CoCrFeNiNb _{0.309} (4d)	fcc+Laves	0.963	19
CoCrFeNiNb _{0.412} (4d)	fcc+Laves	0.990	19
CoCrFeNiZr _{0.05} (4d)	fcc+Ni ₇ Zr ₂	0.899	This work
CoCrFeNiZr _{0.1} (4d)	fcc+Ni ₇ Zr ₂	0.924	This work
CoCrFeNiZr _{0.15} (4d)	fcc+Ni ₇ Zr ₂ +Laves	0.948	This work
CoCrFeNiZr _{0.2} (4d)	fcc+Ni ₇ Zr ₂ +Laves	0.972	This work
CoCrFeNiZr _{0.25} (4d)	fcc+Ni ₇ Zr ₂ +Laves	0.995	This work
CoCrFeNiZr _{0.3} (4d)	fcc+Ni ₇ Zr ₂ +Laves	1.018	This work
CoCrFeNiZr _{0.35} (4d)	fcc+Ni ₇ Zr ₂ +Laves	1.040	This work
CoCrFeNiZr _{0.4} (4d)	fcc+Ni ₇ Zr ₂ +Laves	1.062	This work
CoCrFeNiZr _{0.45} (4d)	fcc+Laves	1.083	This work
CoCrFeNiZr _{0.5} (4d)	fcc+Laves	1.104	This work

^athese two alloys were wrongly classified as fcc solid solution forming HEAs in our previous work,²³ and as a matter of fact they both contain intermetallic compounds.

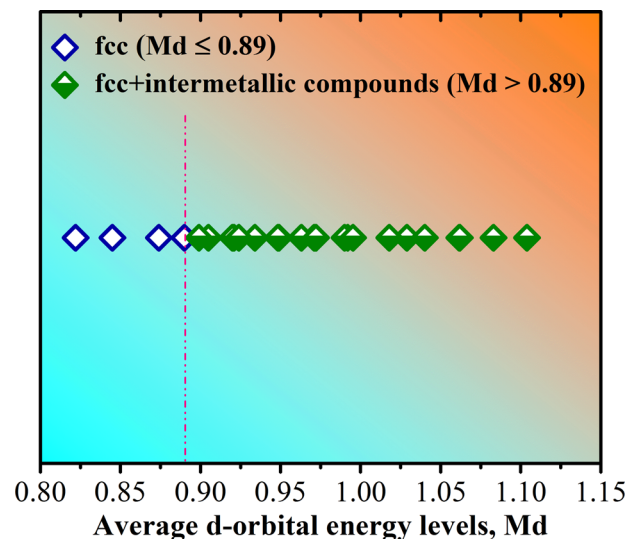


FIG. 7. The parameter Md and its critical role in delineating the phase boundary in CoCrFeNi and CoCrFeNiM_x (M = Zr, Nb, Mo; Ti, Mn, Cu) alloys.

in the alloy, can much better separate the formation of solid solutions and intermetallic compounds, compared to the original approach. The Md parameter, even better than the improved δ - ΔH_{mix} approach, can accurately predict the solid solubility, or the phase boundary between the fcc solid solution and intermetallic compounds, in CoCrFeNiM_x (M = Zr, Nb, and Mo) alloys.

ACKNOWLEDGMENTS

S.S. and S.G. are grateful for the financial support from the Areas of Advance Materials Science from the Chalmers University of Technology. S.G. also acknowledges the partial support from the State Key Laboratory for Advanced Metals and Materials Open Fund at the University of Science and Technology Beijing (2013-Z04).

- ¹J. W. Yeh, S. K. Chen, S. J. Lin, J. Y. Gan, T. S. Chin, T. T. Shun, C. H. Tsau, and S. Y. Chang, *Adv. Eng. Mater.* **6**, 299 (2004).
- ²B. Cantor, I. T. H. Chang, P. Knight, and A. J. B. Vincent, *Mater. Sci. Eng. A* **375–377**, 213 (2004).
- ³D. Miracle and O. Senkov, *Acta Mater.* **122**, 448 (2017).
- ⁴M. C. Gao, J.-W. Yeh, P. K. Liaw, and Y. Zhang, *High-Entropy Alloys: Fundamentals and Applications* (Springer, Cham, Switzerland, 2016).
- ⁵D. B. Miracle, J. D. Miller, O. N. Senkov, C. Woodward, M. D. Uchic, and J. Tiley, *Entropy* **16**, 494 (2014).
- ⁶Y. Zhang, T. T. Zuo, Z. Tang, M. C. Gao, K. A. Dahmen, P. K. Liaw, and Z. P. Lu, *Prog. Mater. Sci.* **61**, 1 (2014).
- ⁷Z. P. Lu, H. Wang, M. W. Chen, I. Baker, J. W. Yeh, C. T. Liu, and T. G. Nieh, *Intermetallics* **66**, 67 (2015).
- ⁸S. Sheikh, S. Shafeie, Q. Hu, J. Ahlström, C. Persson, J. Veselý, J. Zýka, U. Klement, and S. Guo, *J. Appl. Phys.* **120**, 164902 (2016).
- ⁹O. N. Senkov, G. B. Wilks, J. M. Scott, and D. B. Miracle, *Intermetallics* **19**, 698 (2011).
- ¹⁰O. N. Senkov, G. B. Wilks, D. B. Miracle, C. P. Chuang, and P. K. Liaw, *Intermetallics* **18**, 1758 (2010).
- ¹¹F. Granberg, K. Nordlund, M. W. Ullah, K. Jin, C. Lu, H. Bei, L. Wang, F. Djurabekova, W. Weber, and Y. Zhang, *Phys. Rev. Lett.* **116**, 135504 (2016).
- ¹²Y. Zhang, G. M. Stocks, K. Jin, C. Lu, H. Bei, B. C. Sales, L. Wang, L. K. Béland, R. E. Stoller, and G. D. Samolyuk, *Nat. Commun.* **6**, 8736 (2015).
- ¹³C. Lu, T. Yang, K. Jin, N. Gao, P. Xiu, Y. Zhang, F. Gao, H. Bei, W. J. Weber, and K. Sun, *Acta Mater.* **127**, 98 (2017).
- ¹⁴S. Guo, C. Ng, J. Lu, and C. T. Liu, *J. Appl. Phys.* **109**, 103505 (2011).
- ¹⁵Z. Li, K. G. Pradeep, Y. Deng, D. Raabe, and C. C. Tasan, *Nature* **534**, 227 (2016).
- ¹⁶O. N. Senkov, J. M. Scott, S. V. Senkova, D. B. Miracle, and C. F. Woodward, *J. Alloys Compd.* **509**, 6043 (2011).
- ¹⁷B. Gludovatz, A. Hohenwarter, D. Catoor, E. H. Chang, E. P. George, and R. O. Ritchie, *Science* **345**, 1153 (2014).
- ¹⁸S. Guo and C. T. Liu, *Prog. Nat. Sci.: Mater. Int.* **21**, 433 (2011).
- ¹⁹W. H. Liu, J. Y. He, H. L. Huang, H. Wang, Z. P. Lu, and C. T. Liu, *Intermetallics* **60**, 1 (2015).
- ²⁰F. He, Z. J. Wang, P. Cheng, Q. Wang, J. J. Li, Y. Y. Dang, J. C. Wang, and C. T. Liu, *J. Alloys Compd.* **656**, 284 (2016).
- ²¹W. H. Liu, Z. P. Lu, J. Y. He, J. H. Luan, Z. J. Wang, B. Liu, Y. Liu, M. W. Chen, and C. T. Liu, *Acta Mater.* **116**, 332 (2016).
- ²²T. T. Shun, L. Y. Chang, and M. H. Shiu, *Mater. Charact.* **70**, 63 (2012).
- ²³S. Sheikh, U. Klement, and S. Guo, *J. Appl. Phys.* **118**, 194902 (2015).
- ²⁴J. O. Andersson, T. Helander, L. H. Hoglund, P. F. Shi, and B. Sundman, *Calphad* **26**, 273 (2002).
- ²⁵See www.thermocalc.com for detailed description for the software and database TCHEA1.
- ²⁶C. Ng, S. Guo, J. H. Luan, S. Q. Shi, and C. T. Liu, *Intermetallics* **31**, 165 (2012).
- ²⁷C. Ng, S. Guo, J. H. Luan, Q. Wang, J. Lu, S. Q. Shi, and C. T. Liu, *J. Alloys Compd.* **584**, 530 (2014).
- ²⁸C. Zhang, F. Zhang, S. L. Chen, and W. S. Cao, *JOM* **64**, 839 (2012).
- ²⁹J. He, H. Wang, Y. Wu, X. Liu, H. Mao, T. Nieh, and Z. Lu, *Intermetallics* **79**, 41 (2016).
- ³⁰D. Choudhuri, B. Gwalani, S. Gorsse, C. Mikler, R. Ramanujan, M. Gibson, and R. Banerjee, *Scr. Mater.* **127**, 186 (2017).
- ³¹G. Bracq, M. Laurent-Brocq, L. Perrière, R. Pirès, J.-M. Joubert, and I. Guillot, *Acta Mater.* **128**, 327 (2017).
- ³²S. Guo, Q. Hu, C. Ng, and C. T. Liu, *Intermetallics* **41**, 96 (2013).
- ³³S. Guo, *Mater. Sci. Technol.* **31**, 1223 (2015).
- ³⁴Y. Zhang, Y. J. Zhou, J. P. Lin, G. L. Chen, and P. K. Liaw, *Adv. Eng. Mater.* **10**, 534 (2008).
- ³⁵Z. Wang, Y. Huang, Y. Yang, J. Wang, and C. T. Liu, *Scr. Mater.* **94**, 28 (2015).
- ³⁶Y. F. Ye, Q. Wang, J. Lu, C. T. Liu, and Y. Yang, *Mater. Today* **19**(6), 349 (2016).
- ³⁷E. J. Pickering and N. G. Jones, *Int. Mater. Rev.* **61**, 183 (2016).
- ³⁸K. G. Pradeep, C. C. Tasan, M. J. Yao, Y. Deng, H. Springer, and D. Raabe, *Mater. Sci. Eng. A* **648**, 183 (2015).
- ³⁹A. Takeuchi and A. Inoue, *Mater. Trans.* **41**, 1372 (2000).
- ⁴⁰M. S. Lucas, G. B. Wilks, L. Mauger, J. A. Munoz, O. N. Senkov, E. Michel, J. Horwath, S. L. Semiatin, M. B. Stone, D. L. Abernathy, and E. Karapetrova, *Appl. Phys. Lett.* **100**, 251907 (2012).
- ⁴¹Y. J. Hsu, W. C. Chiang, and J. W. Wu, *Mater. Chem. Phys.* **92**, 112 (2005).
- ⁴²C. J. Tong, Y. L. Chen, S. K. Chen, J. W. Yeh, T. T. Shun, C. H. Tsau, S. J. Lin, and S. Y. Chang, *Metall. Mater. Trans. A* **36**, 881 (2005).
- ⁴³T. T. Shun, L. Y. Chang, and M. H. Shiu, *Mater. Sci. Eng. A* **556**, 170 (2012).